


Please cite the Published Version

Alismaeel, Ziad T, Al-Jadir, Thaer M, Albayati, Talib M, Abbas, Ammar S and Doyle, Aidan M  (2022) Modification of FAU zeolite as an active heterogeneous catalyst for biodiesel production and theoretical considerations for kinetic modeling. *Advanced Powder Technology*, 33 (7). p. 103646. ISSN 0921-8831

DOI: <https://doi.org/10.1016/j.ap.2022.103646>

Publisher: Elsevier

Version: Accepted Version

Downloaded from: <https://e-space.mmu.ac.uk/629951/>

Usage rights:  [Creative Commons: Attribution-Noncommercial-No Derivative Works 4.0](https://creativecommons.org/licenses/by-nc-nd/4.0/)

Additional Information: This is an Accepted Manuscript of an article which appeared in *Advanced Powder Technology*, published by Elsevier

Enquiries:

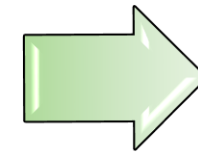
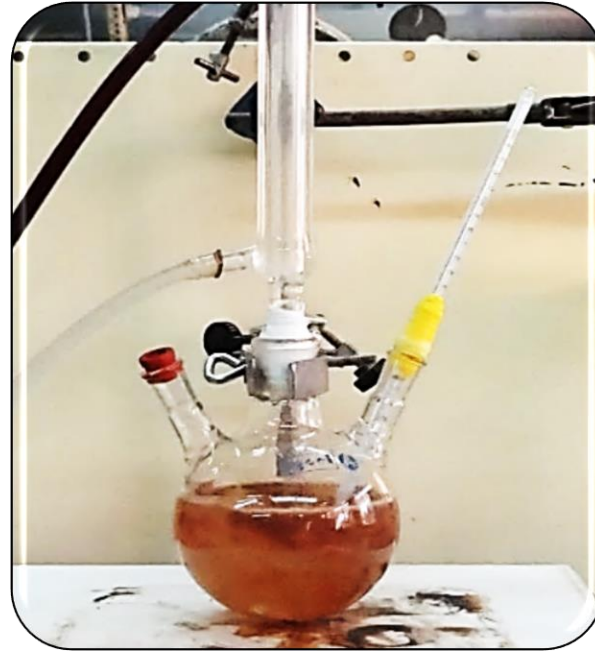
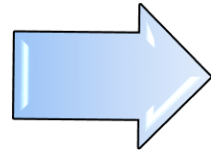
If you have questions about this document, contact openresearch@mmu.ac.uk. Please include the URL of the record in e-space. If you believe that your, or a third party's rights have been compromised through this document please see our Take Down policy (available from <https://www.mmu.ac.uk/library/using-the-library/policies-and-guidelines>)

Advanced Powder Technology

Modification of FAU zeolite as an active heterogeneous catalyst for biodiesel production and theoretical considerations for kinetic modeling

--Manuscript Draft--

Manuscript Number:	ADVPT-D-21-01773R2
Article Type:	Original Research Paper
Keywords:	Biodiesel; Modified Faujasite zeolite; Reaction kinetics models; Transesterification; Heterogeneous reaction.
Corresponding Author:	Talib M. Albayati, Prof. Dr. University of Technology Baghdad, IRAQ
First Author:	Talib M. Albayati, Prof. Dr.
Order of Authors:	Talib M. Albayati, Prof. Dr. Ziad T Alismaeel Thaer M. Al-Jadir Ammar S. Abbas Aidan M. Doyle
Abstract:	<p>In this work, a high purity FAU-type zeolite catalyst was prepared from shale rock and modified as a heterogeneous efficient catalyst for biodiesel production from sunflower oil. The characterization properties for both of the prepared catalysts were determined using X-ray diffraction (XRD), scanning electron microscopy (SEM), energy-dispersive X-ray spectroscopy (EDAX), Brunauer–Emmett–Teller (BET), and Fourier-transform infrared spectroscopy (FTIR). The incipient wetness impregnation method was adopted for loading the catalyst with three base precursors: NaOH, KOH, and Ca(OH)₃. Different factors affecting transesterification reaction onto modified Na-K-Ca-FAU zeolite were investigated such as; temperature (35, 45, 55, and 65°C), catalyst concentrations (2, 3, 4, 5, and 6 wt %) and the molar ratio of methanol to sunflower oil (3:1, 6:1, 9:1 and 12:1). The optimum conditions of transesterification reactions were obtained for reaction time (4 h) and agitation rate (700 rpm) in a batch reactor at 65°C reaction temperature, 5% catalyst concentration, and a 9:1 molar ratio of methanol to oil. The experimental results showed that the conversion of triglyceride in sunflower oil to fatty acid methyl ester (FIME) increased from 48.62 to 91.6% when the FAU zeolite was loaded with 15 wt % of the three bases. The properties of the produced biodiesel were evaluated within the standard performance ASTM D-6751. This study shows that the three base precursors (i.e., NaOH, KOH, and Ca(OH)₃) were successfully loaded onto support FAU zeolite and functioned as excellent catalysts for biodiesel production. Theoretical considerations for kinetic modeling in the heterogeneous transesterification reaction were investigated using MATLAB programming. The experimental and theoretical considerations for kinetic modeling were fitted well.</p>



Irish shale rock to rock
FAU-type zeolite catalyst

Transesterification of
sunflower over FAU-
type zeolite catalyst and
modified versions with
NaOH, KOH, and
 $\text{Ca}(\text{OH})_2$

Biodiesel
characterization and
kinetics study

1
2
3
4 **Modification of FAU zeolite as an active heterogeneous catalyst for biodiesel production**
5
6 **and theoretical considerations for kinetic modeling**
7
8

9 Ziad T. Alismaeel¹, Thaer M. Al-Jadir², Talib M. Albayati^{3*}, Ammar S. Abbas⁴, Aidan M. Doyle⁵

10
11 ¹ Department of Biochemical Engineering, Al-Khwarizmi College of Engineering, University of
12 Baghdad, Al-Jadryah, P.O. Box 47008, Baghdad, Iraq.
13

14
15 ² Environment Research Center, The University of Technology- Iraq.
16

17
18 ³ Department of Chemical Engineering, University of Technology- Iraq, 52 Alsinaa St., PO Box
19 35010, Baghdad, Iraq.
20

21
22 ⁴ Department of Chemical Engineering, College of Engineering, University of Baghdad, Al-
23 Jadryah, P.O. Box 47221, Baghdad, Iraq.
24

25
26 ⁵ Division of Chemistry and Environmental Science, Manchester Metropolitan University, Chester
27 St., Manchester M1 5GD, United Kingdom.
28

29
30
31
32
33 * **Corresponding author:** Talib.M.Naieff@uotechnology.edu.iq
34

35
36 **Abstract**
37

38 In this work, a high purity FAU-type zeolite catalyst was prepared from shale rock and modified
39 as a heterogeneous efficient catalyst for biodiesel production from sunflower oil. The
40 characterization properties for both of the prepared catalysts were determined using X-ray
41 diffraction (XRD), scanning electron microscopy (SEM), energy-dispersive X-ray spectroscopy
42 (EDAX), Brunauer–Emmett–Teller (BET), and Fourier-transform infrared spectroscopy (FTIR).
43
44 The incipient wetness impregnation method was adopted for loading the catalyst with three base
45 precursors: NaOH, KOH, and Ca(OH)₃. Different factors affecting transesterification reaction
46 onto modified Na-K-Ca-FAU zeolite were investigated such as; temperature (35, 45, 55, and
47 65°C), catalyst concentrations (2, 3, 4, 5, and 6 wt %) and the molar ratio of methanol to sunflower
48
49
50
51
52
53
54
55
56
57
58
59
60
61
62
63
64
65

1
2
3
4 oil (3:1, 6:1, 9:1 and 12:1). The optimum conditions of transesterification reactions were obtained
5
6 for reaction time (4 h) and agitation rate (700 rpm) in a batch reactor at 65°C reaction temperature,
7
8 5% catalyst concentration, and a 9:1 molar ratio of methanol to oil. The experimental results
9
10 showed that the conversion of triglyceride in sunflower oil to fatty acid methyl ester (FIME)
11
12 increased from 48.62 to 91.6% when the FAU zeolite was loaded with 15 wt % of the three bases.
13
14 The properties of the produced biodiesel were evaluated within the standard performance ASTM
15
16 D-6751. This study shows that the three base precursors (i.e., NaOH, KOH, and Ca(OH)₃) were
17
18 successfully loaded onto support FAU zeolite and functioned as excellent catalysts for biodiesel
19
20 production. Theoretical considerations for kinetic modeling in the heterogeneous
21
22 transesterification reaction were investigated using MATLAB programming. The experimental
23
24 and theoretical considerations for kinetic modeling were fitted well.
25
26
27
28
29
30

31 **Keywords:** Biodiesel; Modified Faujasite zeolite; Reaction kinetics models; Transesterification;
32
33 Heterogeneous reaction.
34

35 36 **1. Introduction**

37
38 The Immoderate consumption of fossil fuels has led to greenhouse gas emissions and global
39
40 warming, and the available fossil fuel resources will be depleted by 2050 due to their rapid
41
42 exhaustion. Environmental pollution problems caused by exhaust emissions have received
43
44 increasing attention worldwide with the development of society [1]. Biodiesel is considered a
45
46 promising alternative to fossil fuels due to its positive effect on the environment. Biodiesel
47
48 production by transesterification reactions use homogeneous catalysts, such as H₂SO₄, NaOH, and
49
50 KOH to accelerate the reaction over a reasonable amount of time and at moderate temperatures
51
52 [2,3]. However, these homogeneous catalysts are not environmentally friendly because they
53
54 produce a huge amount of wastewater when the glycerol and biodiesel are washed. Therefore,
55
56
57
58
59
60
61
62
63
64
65

1
2
3
4 heterogeneous catalysts are required for biodiesel production due to their advantages over
5
6 homogeneous catalysts, including reusability, easy separation of biodiesel from glycerol, and a
7
8 lower energy requirement [4,5]. In addition, little or no wastewater is produced during the reaction,
9
10 which occurs with a minimal consumption of water [6]. Therefore, more recent research efforts
11
12 have focused on the development and testing of heterogeneous catalysts [7, 8]. Researchers are
13
14 interested in employing nanocatalysts in transesterification because of their properties compared
15
16 to microscopic catalysts [9]. Nanocatalysts exhibit very high activity, large pore size, reactivity,
17
18 and large surface area [10]. The active surface area is a key property of catalysts [11]. An increase
19
20 in the surface of the catalyst reduces the required amount of the catalyst. Currently, nanocatalysts
21
22 are used for biodiesel synthesis, including Al-Sr [12], $K_2O/\gamma-Al_2O_3$ [13], $Ca/Fe_3O_4@SiO_2$ [14],
23
24 mixed oxide SiO_2/ZrO_2 [15], La_2O_3 [16], NaY zeolite [17 &18], HY-zeolite [19], MCM-48 [20],
25
26 13X-Zeolite and its derivative [21& 22], CaO [23], and manganese doped zinc oxide [24].
27
28
29
30
31
32

33 Numerous studies have reported on the use of heterogeneous catalysis for biodiesel
34
35 production using various feedstocks. However, limited information is available with respect to the
36
37 kinetics and mass transfer studies on the methanolysis process [25-34]. A detailed and genuine
38
39 kinetic heterogeneous catalysis survey should estimate the dominance of the mass transfer
40
41 diffusional resistances and evaluate the reaction rate constants [25]. The rate of the
42
43 transesterification reaction by a heterogeneous catalyst depends on the internal and external
44
45 diffusion of the reactant, surface reaction, reactant adsorption on the catalyst surface, product
46
47 desorption, product external diffusion, and product internal diffusion [33]. Among these
48
49 resistances, for efficient production, it is necessary to evaluate the controlling resistance so as to
50
51 eliminate it. Al-Sakkari et al. (2017) [34] investigated soyabean oil methanolysis kinetics using
52
53
54
55
56
57
58
59
60
61
62
63
64
65

1
2
3
4 cement clinker as a catalyst in a batch reactor and found that the internal and external mass transfer
5
6 resistances were negligible.
7

8
9 Biodiesel synthesis is controlled by surface reactions, which are well explained by the Eley–Rideal
10 (ER) model equation [26], which also explains the kinetics of the basic heterogeneous catalyst.
11
12 However, ER mechanism is not suitable for a catalyst because it leaches into the reaction mixture
13
14 as the mixture becomes partially heterogeneous [27,34]. Additionally, Hsieh et al. (2010) proposed
15
16 that a Langmuir–Hinshelwood model equation described the synthesis of biodiesel using a Ca-
17
18 based heterogeneous catalyst in a continuous reactor [27]. They found that methanol and
19
20 triglyceride adsorption on the catalyst surface, which is then followed by a series of reactions,
21
22 comprises the rate-limiting steps [27]. Hsieh et al. found that the mechanism can be explained by
23
24 first- or second-order homogeneous model equations [27]. Dossin et al. (2006) reported that
25
26 methanol adsorption on the basic active sites is the controlling step [28]. Initially, it forms a
27
28 methoxide anion, which is followed by surface reaction between the triglyceride and methoxide to
29
30 form a tetrahedral intermediate. The complete mechanism is explained by the three-step intrinsic
31
32 ER model equation [29].
33
34
35
36
37
38
39

40
41 The present study was conducted using two catalysts in the transesterification of sunflower
42
43 oil with methanol: a Faujasite zeolite type HY (FAU-type) and a novel modified Faujasite zeolite (
44
45 Na-K-Ca-FAU). The physicochemical properties of the FAU zeolite and modified Faujasite
46
47 zeolite (Na-K-Ca-FAU) catalysts were described by XRD, Brunauer–Emmett–Teller (BET)
48
49 surface area, Scanning Electron Microscope (SEM), energy-dispersive X-ray spectroscopy
50
51 (EDAX) and Fourier-transform infrared spectroscopy (FTIR). Different conditions that effecting
52
53 on transesterification reaction were studied such as reaction temperature, catalyst concentration
54
55 and methanol/oil molar ratio. In addition, the kinetic parameters for the transesterification of
56
57
58
59
60
61
62
63
64
65

1
2
3
4 sunflower using a novel modified Faujasite zeolite loaded with NaOH, KOH, and Ca(OH)₂ were
5
6 explored and compared to the literature. The theoretical considerations for kinetic modeling in
7
8 transesterification reaction model was investigated using MATLAB programming.
9

10 11 **2. Experiment**

12 13 **2.1. Materials**

14
15 Shale was gathered from the surface of a tilled field in Ireland's Wexford County. Then,
16
17 the shale was water-washed to eliminate all soil remains. After that, it was dried for about 3 h at
18
19 120°C. Sunflower oil was bought from a local British market in the UK. Sodium hydroxide
20
21 (NaOH) pellets were obtained from Scharlab (Spain). Sodium silicate (Na₄SiO₄) with 99% purity
22
23 was obtained from BDH Chemicals Ltd. (England). Ammonium chloride (NH₄Cl), methanol
24
25 (CH₃OH), phenolphthalein 2% in ethanol, and potassium hydroxide (KOH) were purchased from
26
27 Sigma Aldrich (England). Calcium hydroxide (Ca(OH)₂) 95% (Alfa Aesar, location) and glycerol
28
29 (Sigma Aldrich) were purchased for gas chromatography/flame ionization detector (GC/FID)
30
31 analysis. All standards and reference substances were purchased from Sigma Aldrich as 1,3-di[*cis*-
32
33 9-octadecenoyl] glycerol (diolein); glycerol; 1,2,4-Butanetriol; 1-mono [*cis*-9-octadecenoyl]-*rac*-
34
35 glycerol (monoolein), 1,2,3-tri-[*cis*-9-octadecenoyl] glycerol (triolein), N-Methyl-N-
36
37 (trimethylsilyl)trifluoroacetamide (MSTFA), pyridine; and heptane (Fisher Scientific, England).
38
39
40
41
42
43
44
45

46 47 **2.2. Catalyst preparation**

48
49 The HY (FAU-type) and novel modified Na-K-Ca-FAU zeolites were prepared according
50
51 to a procedure illustrated in our previous papers [35-37]. The procedure included crushing the
52
53 washed shale utilizing a ball mill instrument. It was then sieved at < 90 μm and calcinated for
54
55 approximately 4 h at 800°C in the air to avoid any organic materials. The calcined shale (10 g)
56
57 was refluxed with 40 mL of 5 M HCl at 85°C for 4 h to remove Fe. Filtration was used to recover
58
59
60
61
62
63
64
65

1
2
3
4 the product. Next, 1.5 parts (by mass) of 40 wt % aqueous NaOH solution was mixed with 1 part
5
6 (by mass) of calcined shale. The shale was then cooked in an air furnace for 3 h at 850°C to produce
7
8 fused shale. After cooling to ambient temperature, it was crushed to form a powder. A mixture of
9
10 2 g fused shale, 1 g sodium silicate, and 16 g purified water was poured into a polypropylene
11
12 bottle. The blend was then swirled for 3 h at room temperature, after which it was aged under static
13
14 settings for about 18 h at room temperature. Finally, the combination was hydrothermally treated
15
16 for 24 h at 100°C. Filtration was used to recover the product. To transform prepared Na⁺ zeolite
17
18 into an NH₄⁺ form, 90 g of zeolite was mixed with 250 mL of 2 M ammonium chloride. The mixture
19
20 was stirred for 2 h at room temperature in a round-bottom flask. The solid was recovered using
21
22 filtration. The ion-exchange procedure was conducted twice, using 60 g and 30 g. Finally, it was
23
24 dried for 12 h at 120°C and calcined in air at 500°C for about 4 h. This was performed to produce
25
26 zeolite in H⁺ form, which will be referred to as H-FAU. Before alkali loading, the zeolite was
27
28 dehydrated at 110°C for 2 h in an oven to remove any absorbed water. Then, using the incipient
29
30 wetness method, the bases (i.e., NaOH, KOH, and Ca(OH)₂) were added to the zeolite. Next,
31
32 impregnation solutions were prepared by dissolving the appropriate masses of the NaOH, KOH,
33
34 and Ca(OH)₂ precursors in deionized water, and these solutions were added to the zeolite to create
35
36 loadings of 5 wt.% of each base. After impregnation, the catalysts were dried overnight at ambient
37
38 temperature, heated for 24 h at 120°C, and then calcined in air at 500°C for 4 h to produce an Na-
39
40 K-Ca-FAU catalyst.

51 **2.3. Catalyst characterization**

52
53 A Malvern Panalytical X'Pert powder diffractometer with Cu(K α) 1.5406 Å was used to
54
55 perform XRD at ambient conditions. All powder diffraction patterns were recorded from 4 to 50°
56
57 with a step size of 0.026° and a step time of 50 s using an X-ray tube operating at 40 kV and 30
58
59
60
61
62
63
64
65

1
2
3
4 mA with a fixed 1/4° anti-scatter slim. Nitrogen adsorption/desorption amounts were performed
5
6 using a Micromeritics ASAP 2020 surface analyzer at -196°C. Before analysis, the samples were
7
8 degassed under vacuum (5-10 mbar) for 12 h at 350°C. The samples' BET surface areas were
9
10 measured in the relative pressure range of 0.05-0.30. A JEOL JSM-5600LV scanning electron
11
12 microscope was used to capture SEM images. Energy-dispersive X-ray spectroscopy (EDAX) was
13
14 used to conduct semi quantitative chemical analysis with an Oxford Instruments detector. Also,
15
16 chemical bonds (functional groups) were analyzed and specified by the FTIR spectrometer
17
18 (Nicolet 380).
19
20
21
22

23 **2.4. Catalyst testing**

24 **2.4.1. Batch reactor**

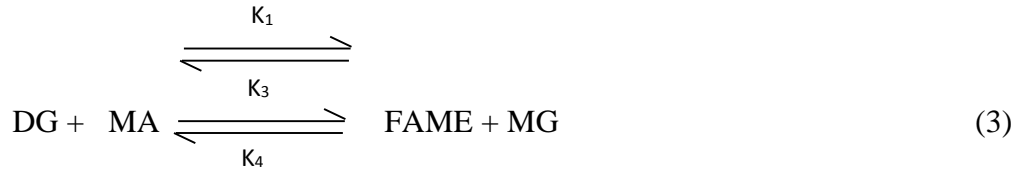
25
26
27
28 The transesterification of sunflower oil with methanol using H-FAU and Na-K-Ca-FAU
29
30 catalysts was performed in the batch reactor. The transesterification reaction was carried out at
31
32 optimum operating conditions: 65°C, 9:1 (methanol: oil molar ratio), and 5 wt.% of each catalyst
33
34 loading to oil. These conditions were chosen after testing different conditions with starting value
35
36 based on a literature review [38]. For example, following the process described by Encinar et al.
37
38 (2010), the catalyst was mixed with methanol, while the sunflower oil was placed in a 500-ml
39
40 three-necked round-bottom flask and heated to 65°C. Next, the catalyst and methanol mixture were
41
42 added to the sunflower oil [38]. Then, every 15 min, 10 ml of the sample (i.e., reaction product)
43
44 was taken from the mixture. These samples were immediately placed in ice containers to stop the
45
46 reaction. The samples were withdrawn at the following times; 30, 60, 90, 120, 150, 180, 210, and
47
48 240 min. Finally, the yield of biodiesel production was calculated according to Eq. (1) from Viele
49
50 et al. (2014) [39].
51
52
53
54
55
56

$$57 \text{Yield} = \frac{\text{wt. of biodiesel production}}{\text{wt. of oil used}} \quad (1)$$

58
59
60
61
62
63
64
65

1
2
3
4 **2.4.2 Theoretical considerations for kinetic modeling**
5

6 The most common mathematical models to study the kinetics of heterogeneity are LH and
7 ER [40]. LH model assumes that the bimolecular reaction between two molecules of the reactant
8 species adsorb on neighboring sites and that the solid catalysts contain Lewis's acid/base sites
9 [41,42]. The ER model assumes that the reaction occurs between a chemisorbed molecule and a
10 non-absorbed molecule from the bulk phase [43]. A solid catalyst leached into the reaction media
11 cannot be considered heterogeneous because its reaction mechanism is similar to homogeneous
12 transesterification [44]. Most researchers have found that triglyceride transesterification occurs in
13 three steps, as expressed in the following equations [12, 14, 17, and 42]:
14
15
16
17
18
19
20
21
22
23
24



40
41 Overall reaction:



50 Where MA is methanol; TG is triglyceride; DG is diglyceride; MG is monoglyceride; and GL is
51 glycerol.
52

53
54 **2.4.3. Sample analysis**
55
56
57
58
59
60
61
62
63
64
65

1
2
3
4 To calculate the triglyceride conversion, the sample withdrawn from the transesterification
5 reaction was used without separating glycerol. The sample was evaluated using a gas
6 chromatography/flame ionization detector (GC/FID). This detector is equipped with an on-column
7 injector, as illustrated in British standards (BS EN 14105 method). This method was used to
8 determine the amounts of mono-, di-, and triglyceride as well as the total glycerol. For GC/FID
9 analysis, stock solutions for different reference substances (i.e., glycerol, monoolein, diolein, and
10 triolein) were prepared by adding pyridine. Three different calibration solutions from these stock
11 reference standards were prepared (S1-S3) to obtain a calibration curve for each substance by
12 mixing them in the vial with 80 µl of internal standards: (1) 1,2,4-Butanetriol (IS1) and 100 µl of
13 internal standards and (2) tricaprin (IS2). After mixing these reference substances with the internal
14 standards, 100 µl of N-Methyl-N-(trimethylsilyl)trifluoroacetamide (MSTFA) was added to the
15 three calibration solutions. Then, the vials were sealed, vigorously shaken, and stored for 15 min
16 at room temperature. Finally, 8 ml of heptane was added. The calibration solutions were ready for
17 analysis after withdrawing 1 µl for the standards (S1-S3) and injecting this onto the GC column.
18 These standards were injected twice (duplicate testing) to increase the reliability of the analysis.
19 Each sample's mass calculations (M) for glycerol, monoglyceride, diglyceride, and triglyceride
20 were analyzed according to Eqs. (6) to (9).
21
22
23
24
25
26
27
28
29
30
31
32
33
34
35
36
37
38
39
40
41
42
43
44

$$\frac{M_{(GL)}}{M_{(is1)}} = a_{(GL)} * \left[\frac{A_{(GL)}}{A_{(is1)}} \right] + b_{(GL)} \quad (2)$$

$$\frac{M_{(MG)}}{M_{(is2)}} = a_{(MG)} * \left[\frac{A_{(MG)}}{A_{(is2)}} \right] + b_{(MG)} \quad (3)$$

$$\frac{M_{(DG)}}{M_{(is2)}} = a_{(DG)} * \left[\frac{A_{(DG)}}{A_{(is2)}} \right] + b_{(DG)} \quad (4)$$

$$\frac{M_{(TG)}}{M_{(is2)}} = a_{(TG)} * \left[\frac{A_{(TG)}}{A_{(is2)}} \right] + b_{(TG)} \quad (5)$$

The mass of the fatty acid methyl ester (FAME) and methanol were determined using Equations (2) - (4).

3. Results and Discussion

3.1. Characterization

The Faujasite HY structure was confirmed by the XRD patterns for the H-FAU produced from shale. Since these have already been argued elsewhere [36], the two configurations of the catalysts (i.e., H-FAU and (K-Na-Ca)-HY-shale zeolites) are shown in **Figure 1**.

Figure 1: XRD Patterns of two Configurations of HY-shale Zeolite

According to this figure, the catalyst modification did not affect the crystallinity phases. However, because the alkali loading was substantially larger (15% by weight), the crystallinity degree of the H-FAU was reduced by 43.12% (10900 to 62000 for the greatest peak at intercept (1, 1, 1), as shown in **Figure 1**. However, all configurations had the same XRD patterns. This is a good indicator that the impregnation procedures worked well because the particle's catalyst maintained the same diffraction pattern throughout the process and did not become amorphous or experience altered diffraction patterns after the modifications.

As demonstrated in **Table 1**, incipient wetting with Ca(OH)₂, NaOH, and KOH bases as well as calcination in the air followed by heating, reduced the BET surface area of the H-FAU from 571 m²g⁻¹ to 325.5 m²g⁻¹. This decrease in the BET surface area was predictable, as the (K-Na-Ca)-HY-shale had undergone a loading basis in the pores of the H-FAU, resulting in some metastable zeolite porosity loss that the high surface area retains.

Table (1): Physicochemical Properties of two HY-shale Zeolite Configurations

1
2
3
4 **Figure 2** illustrates the micron-sized particles of Na-K-Ca-FAU and H-FAU in the SEM images,
5 which were approximately 2 μm , of Na-K-Ca-FAU and H-FAU. The EDAX confirmed the
6 presence of calcium, potassium, sodium, aluminum, and silicon in the underlying zeolite. Also,
7 the FTIR test showed the functional group before and after adding zeolite as shown in **Figure 3**.
8
9 From this figure it can be observed that, a strong bands between 1000 to 1100 cm^{-1} could be
10 assigned to asymmetric stretching vibration modes of internal Si–O bonds in SiO_4 or Al–O bonds
11 in AlO_4 tetrahedral and this is in good agreement with data proposed by [45], and also the
12 stretching Si–OH bond was appeared in the wide range bands at approximately 3500 to 3800 cm^{-1}
13 ¹, and a characteristic bands in the infrared region between 2325 to 2375 cm^{-1} was attributed to the
14 stretching vibration of P–H bond (phosphorus acid). Other bands appear in a wide range near 650
15 to 850 cm^{-1} band is assigned to the stretching vibration modes of O–Si–O or O–Al–O groups. These
16 results are comparable with the results obtained by many researchers such as [46].
17
18
19
20
21
22
23
24
25
26
27
28
29
30
31
32

33 **Figure 2:** SEM and EDAX images for H-FAU (top) and Ca-Na-K-FAU (bottom).
34

35 **Figure 3:** FTIR test for HY-shale (top) and (K-Na-Ca)-HY-shale (bottom).
36
37
38
39
40

41 **3.2. Transesterification reactions**

42
43 The transesterification of sunflower oil with methanol was used as a testing reaction to
44 evaluate the catalytic activity of the shale zeolite. The transesterification is comprised of three
45 consecutive reversible reactions. An extra methanol amount of 9:1 methanol to oleic acid molar
46 ratio was employed to improve the conversion based on studying different molar ratio.
47
48
49
50
51

52
53 The constants “a” and “b” for glycerol and bound glycerides, respectively, were calculated
54 from the calibration curves using BS EN 14105 methods with the GC/FID instrument. The results
55 are shown in **Table 2**.
56
57
58
59
60
61
62
63
64
65

Table (2): The Constant Values of all Types of Oils

Then, for each sample, the mass (M) calculation for these components was analyzed according to Eqs. 10-13 for glycerols, monoglycerides, diglycerides, and triglycerides, respectively.

$$\frac{M_{(GL)}}{M_{(is1)}} = 0.909 * \left[\frac{A_{(GL)}}{A_{(is1)}} \right] - 0.010 \quad (6)$$

$$\frac{M_{(MG)}}{M_{(is2)}} = 0.723 * \left[\frac{A_{(MG)}}{A_{(is2)}} \right] + 0.281 \quad (7)$$

$$\frac{M_{(DG)}}{M_{(is2)}} = 0.956 * \left[\frac{A_{(DG)}}{A_{(is2)}} \right] + 0.013 \quad (8)$$

$$\frac{M_{(TG)}}{M_{(is2)}} = 2.667 * \left[\frac{A_{(TG)}}{A_{(is2)}} \right] + 0.038 \quad (9)$$

Figures 4 and 5 show the concentration of glycerides, monoglycerides, diglycerides, triglycerides, methanol, and FAME versus time for the H-FAU and Na-K-Ca-FAU zeolites, respectively.

Figure 4: Concentration-Time Plot for Transesterification Using H-FAU Zeolite

From figure 4, it can be inferred that after 4 h of utilizing H-FAU as a catalyst, the triglyceride conversion in the transesterification reaction was 48.62%. This relatively low percentage of triglyceride conversion might be due to its large molecular size compared to the small pore diameter of H-FAU zeolite [47]. Therefore, the larger size might restrict the triglyceride molecules from reaching the active site inside the pore of the catalyst, as suggested by Endalew et al. (2011) [47]. Their study explained the reasons for the lower conversion of triglyceride in using zeolites as catalysts in transesterification reactions without adjustments. The same outcomes were

1
2
3
4 compatible with those obtained by Najafpour et al. (2014) [48], who achieved the maximum value
5
6 of triglyceride conversion (46 %, after 6 h) using powdered zeolite produced from a kaoline source.
7
8 The reaction conditions were 5:1 molar ratio methanol: wet catalyzed oxidation (WCO) and a
9
10 temperature of 70°C. Furthermore, Noiroj et al. (2009) proposed that zeolites' thin pore size limits
11
12 their ability to be catalysts in transesterification reactions due to the triglyceride's limited
13
14 adsorption on the active sites [49].
15
16
17
18

19 **Figure 5: Concentration-Time Plot for Transesterification using Na-K-Ca-FAU Zeolite**

20
21 **Figure 5** shows that the triglyceride conversion in the transesterification reaction was 91.6% after
22
23 4 h when utilizing Na-K-Ca-FAU as a catalyst. This relatively high conversion percentage can be
24
25 credited to the excellent adjustment of the H-FAU zeolite which present in large amounts during
26
27 the basic was loading (15 wt %) of NaOH, CaOH, and KOH over the H-FAU zeolite, which is
28
29 preferred for transesterification reactions.
30
31
32

33
34 Following the purification of the product with distilled water and separation of the
35
36 unreacted catalyst, glycerol, and methanol, the yield of the transesterification process was 89.37%.
37
38 These outcomes are very close to those obtained by Noiroj et al. (2009) [49]. In addition, Noiroj
39
40 et al. revealed that 3.18% of the loaded K leached into the reaction mix [49]. However, they stated
41
42 that this amount of leaching does not influence catalyst activity because it is equal to the amount
43
44 that exists in the original catalyst [49].
45
46
47

48 **3.2.1 Effect of reaction temperature on transesterification reactions**

49
50 The transesterification of sunflower oil with methanol was carried out at 35, 45, 55 and 65
51
52 °C, in order to determine the temperature influence on the methyl esters production.
53
54

55 Figure (6) shows the fatty acid methyl ester content with different temperatures: 35, 45, 55 and
56
57 65°C for four hours, using fixed amount for both methanol/oil molar ratios equal to 9:1 and 5 wt
58
59
60
61
62
63
64
65

1
2
3
4 % Na-K-Ca-FAU catalyst with respect to sunflower oil, these two values were selected as initial
5
6 conditions since in literature review many researchers recommended these values such as [38].
7
8

9 **Figure 6:** Effect of Temperature on FAME Content using Catalyst Concentration 5% and
10
11 meth/oil 9:1
12
13

14 It is obviously from figure 6, the content of fatty acid methyl ester increase with increasing
15
16 temperature, for instance, the conversion of sunflower oil at 35°C is about 43.2 % after 240 min,
17
18 while the conversion of sunflower oil at 65°C and the same time is about 91.6 %, and these results
19
20 are expected, since the increase in temperature leads to increase in molecular activity (i.e. more
21
22 molecules have energy to overcome the energy barrier of the reaction and react easily) According
23
24 to the collision theory, the famous theory, that depicted the chemical reaction [50].
25
26
27

28 **3.2.2 Effect of catalyst concentration on transesterification reactions**

29
30 In order to examine the activity of modified Na-K-Ca-FAU zeolite catalyst, a variety of
31
32 weight percent of catalyst to oil were used in transesterification reaction of sunflower oil with
33
34 methanol. Reactions were carried out at a constant temperature of 65 °C, and using a fixed
35
36 methanol/oil molar ratio of 9:1. An excessive amount of methanol was used here because the
37
38 reaction is reversible. Figure (7) shows the effect of different weight percent ratios of modified
39
40 Na-K-Ca-FAU zeolite to oil; 2, 3, 4, 5 and 6 wt% on the transesterification reaction.
41
42
43
44

45
46 As seen in the figure (7), the transesterification reaction of sunflower oil is directly
47
48 proportion with amount of catalyst loading (Na-K-Ca-FAU zeolite), and this case is anticipated
49
50 since the increase in catalyst amount means increase in number of active site on which the
51
52 transesterification reaction took place, so, the maximum conversion has been reached when
53
54 maximum amount of catalyst was loaded (i.e. 6 % loading), this conversion was about 91.8 % after
55
56 4 hours, but the percentage increase in conversion was not remarkable when comparing with the
57
58
59
60
61
62
63
64
65

1
2
3
4 conversion obtained by loading catalyst 5 % , since the conversion at these amount was attained
5
6 about 91.6%, These results are a good agreement to the other reports [51] that mentioned the
7
8 increasing of catalyst amount beyond 5.27% did not have much effect on transesterification
9
10 reaction.
11
12

13
14 **Figure 7:** Effect of catalyst Concentration on FAME Content using meth/oil =9:1 and
15
16 Temperature 65C°
17
18

19 **3.2.3 Effect of methanol/oil molar ratio on transesterification reactions**

20
21 Transesterification of sunflower oil with methanol is a reversible reaction with a
22
23 stoichiometry methanol/oil molar ratio of 3:1. An excess amount of methanol is usually used to
24
25 obtain better conversion. Unreacted methanol must be recycled for reuse and a large amount of
26
27 energy is needed. Hence, the optimal methanol/oil molar ratio is to be determined as the best
28
29 possible of energy saving and the best reaction conversion is considered. Four methanol/oil molar
30
31 ratios were used in transesterification reactions 3:1, 6:1, 9:1 and 12:1 with fixed concentration of
32
33 5 wt % Na-K-Ca-FAU catalyst at 65°C for 4 hours in batch reactor as shown in figure (8).
34
35
36
37

38 **Figure 8:** Effect of meth/oil on FAME Content using Catalyst Concentration 5% and
39
40 Temperature 65C°
41
42

43 From figure (8), it can be seen the significant increase in fatty acid methyl ester content when
44
45 methanol/oil molar ratio increase from 3:1 to 9:1, but it was slightly decreased in fatty acid methyl
46
47 ester content when increasing methanol/oil molar ratio from 9:1 to 12:1. The higher alcohol molar
48
49 ratio interferes with the separation of glycerol because there is an increase in solubility. In addition,
50
51 an excess of alcohol seems to favor conversion of diglyceride to monoglyceride, but there also is
52
53 a slight recombination of esters and glycerol to monoglyceride because their concentration keeps
54
55
56
57
58
59
60
61
62
63
64
65

1
2
3
4 increasing during the course of the reaction, in contrast to reactions conducted with low molar
5 ratios [52].
6
7

9 3.3. Kinetic study for transesterification

10 The kinetic parameters of the sunflower oil transesterification reactions (Eq. (2) to (4))
11 (i.e., $k_1, k_2, k_3, k_4, k_5,$ and k_6) were determined using computer programs developed by the authors
12 to solve six nonlinear differential equations. MATLAB language was employed to construct the
13 program. The MATLAB programs used to calculate the reaction rate constants and study the
14 simulated data's dynamic behavior were based on Titipong (2011) [53] but were modified to be
15 suitable for the current work. The solution of the differential equations (14 to 19) was obtained
16 using the built-in MATLAB command "ode45".
17
18
19
20
21
22
23
24
25
26
27

$$28 \quad r_{TG} = \frac{d[TG]}{dt} = -k_1 [TG][MA] + k_2 [DG][FAME] \quad (10)$$

$$29 \quad r_{DG} = \frac{d[DG]}{dt} = k_1 [TG][MA] + k_4 [MG][FAME] - k_2 [DG][FAME] - k_3 [DG][MA] \quad (11)$$

$$30 \quad r_{MG} = \frac{d[MG]}{dt} = k_3 [DG][MA] + k_6 [GL][FAME] - k_4 [MG][FAME] - k_5 [MG][MA] \quad (12)$$

$$31 \quad r_{FAME} = \frac{d[FAME]}{dt} = k_1 [TG][MA] + k_3 [DG][MA] + k_5 [MG][MA] - k_2 [DG][FAME] \quad (13)$$

$$32 \quad -k_4 [MG][FAME] - k_6 [GL][FAME]$$

$$33 \quad r_{GL} = \frac{d[GL]}{dt} = k_5 [MG][MA] - k_6 [GL][FAME] \quad (14)$$

$$34 \quad r_{MA} = \frac{dMA}{dt} = -\frac{d[FAME]}{dt} \quad (15)$$

35 where r_i represents the formation rates of species i (mol/L. time); i represents the species
36 concentration i (mol/L); and k_i represents the rate constant of the individual transesterification
37 reactions for species i (L/mol. time).
38
39
40
41
42
43
44
45
46
47
48
49
50
51
52
53
54
55
56
57
58
59
60
61
62
63
64
65

1
2
3
4 The difference between the experimental and calculated values was defined as Eq. (20).
5

$$C_{error} = ABS(C_{cal} - C_{exp}) \quad (16)$$

6
7
8
9 where C_{cal} is a matrix used to store output values from the calculation results, and C_{exp} is a matrix
10 used to store output values from the experimental results.
11
12

13
14 Lastly, the founded value of the constants is displayed in **Table 3**.
15

16
17 **Table (3):** Optimal Value of the Constants for Transesterification Rate Reaction
18

19 These values were utilized to simulate the reaction products' dynamic behavior and compare that
20 with the experimental behavior for different components. The simulations and comparisons for
21 triglyceride, diglyceride, monoglyceride, methyl ester, glycerol, and methanol concentrations are
22 shown in Figures 9 (a-f), respectively. **Table 3** shows that the order of the forward reactions rate
23 constants ($k_1 < k_3 < k_5$) is compatible with the outcomes obtained from the transesterification of
24 soybeans reported by Nouredini and Zhu (1997) [30]. In contrast, the order of the backward
25 reaction rate constants was ($k_6 < k_4 < k_2$) in the current study, which is compatible with the results
26 achieved by Klofutar and Golob (2010) [32]. From the results displayed in Figures 9 (A-F), it can
27 be inferred that the simulated data acquired from the estimated constants (k_1 to k_6) of the reaction
28 rate is very similar to the experimental data. In fact, this is more pronounced in the concentrations
29 of triglyceride, methyl ester, glycerol, and methanol, as shown in Figures 9 (A, B, C, D, E, and F),
30 respectively. These results suggest that the reaction rate constants are consistent and can simulate
31 the experimental results.
32
33
34
35
36
37
38
39
40
41
42
43
44
45
46
47
48
49
50
51
52
53
54
55

56 **Figure 9:** Dynamic Behavior Comparison between Experimental Work and Simulated Data for
57
58 Different Product Concentrations
59
60
61
62
63
64
65

1
2
3
4 (A) For Triglyceride Concentration: (B) For Diglyceride Concentration: (C) For Monoglyceride
5
6 Concentration: (D) For Methyl Ester Concentration: (E) For Glycerol Concentration: (F) For
7
8 Methanol Concentration.
9

10 11 12 13 14 **3.4 Characterization of biodiesel from sunflower oil transesterification**

15
16 Product characteristics are vital because they help in examining the validity of the
17 reactions. Therefore, experimental sets were employed on the biodiesel produced from the
18 transesterification of sunflower oil. Using (Na-Ca-K)-HY-shale zeolite as a catalyst produced the
19 highest triglyceride conversion (91.6%). The results of various tests of this biodiesel are listed in
20
21 **Table 4** and compared to results obtained by Arjun et al. (2008) [54].
22
23
24
25
26
27

28
29 **Table (4): Specification of the Biodiesel Production**

30
31 The viscosity of the biodiesel in the present work was 4.3 mm²/s when using the transesterification
32 reactions. This value is adequate because it is within the range of the ASTM standard (1.9-6
33 mm²/s). However, the specific gravity was 0.91. This number was slightly higher than the range
34 specified by the ASTM. Such a result led to calculating the American Petroleum Institute (API)
35 gravity value to be 23.99 degrees because the reversible proportion was between the API degree
36 and the specific gravity. The biodiesel flashpoint in the present work was 151°C. This value lay
37 within the range of 100-170 of the ASTM. It also suggests the viability of using biodiesel (B100)
38 in a diesel engine as it is environmentally safe. For the present work, the biodiesel's cetane number
39 was about 57.6. In comparison, it was 61 for the biodiesel obtained from WCO by Arjun et al.
40 [54]. Oils and fats include large quantities of saturated and unsaturated free fatty acids as well as
41 triglycerides. Saturated components oxidize at a slower rate than unsaturated components. Using
42 ethyl alcohol to produce biodiesel is favorable due to the presence of an extra carbon atom in the
43
44
45
46
47
48
49
50
51
52
53
54
55
56
57
58
59
60
61
62
63
64
65

1
2
3
4 ethanol molecule, which increases the heat content and the cetane number, according to Vicente
5
6
7 et al. (2007) [55].
8

9 The present work's cloud point and pour point of biodiesel were 2 and -3, respectively,
10
11 higher than those obtained for diesel fuel, matching the findings presented by Arjun et al. (2008)
12
13 [54]. Arjun et al. Suggested that the ethyl ester's cloud point decreased by 2 degrees when using
14
15 methyl ester. The cloud points of the fatty acid ethyl esters of canola oils, linseed, rapeseed, and
16
17 sunflower were -1, -2, -2, and -1°C, respectively, according to Lang et al. (2001) [56]. On the
18
19 other hand, the cloud points of the related FAMES were 1, 0, 0, and 1°C, respectively [56].
20
21
22

23 The weight percentage of the carbon residue in the biodiesel in the present work was
24
25 0.0832, which was higher than the standard value. Such an increase in the carbon residue can be
26
27 attributed to the long chain of carbons found in triglycerides, which leads to an increased carbon
28
29 residue. Beatrice et al. (2014) revealed that that for biodiesel produced by the transesterification
30
31 of already used vegetable oil, the value of the carbon residue was 0.18. This value was higher than
32
33 the one for the biodiesel produced by the current study [57].
34
35
36
37

38 **4. Conclusions**

39

40 Shale is a good source of FAU-type zeolite for the catalyzed transesterification of
41
42 sunflower oil and methanol for biodiesel production. The physicochemical properties of both the
43
44 FAU zeolite and the modified Faujasite zeolite (Na-K-Ca-FAU) catalysts were characterized
45
46 successfully. The inclusion of three bases (i.e., NaOH, KOH, and Ca (OH)₂) to the zeolite can
47
48 significantly increase the transesterification conversion of sunflower oil. The optimum conditions
49
50 for operating parameters of transesterification reactions were obtained in a batch reactor at: 65°C
51
52 reaction temperature, 5% catalyst concentration, and a 9:1 molar ratio of methanol to oil. The
53
54 kinetic parameters can be calculated easily using MATLAB software. The experimental and
55
56
57
58
59
60
61
62
63
64
65

1
2
3
4 theoretical considerations for the kinetic modeling fit well. The findings prove the appropriateness
5
6 of using Na-K-Ca-FAU as a heterogeneous active catalyst for biodiesel production.
7
8
9

10 11 12 13 14 **References**

15
16 [1] Yusra A. Abd Al-Khodor, Talib M. Albayati, (2020). Employing sodium hydroxide in
17
18 desulfurization of the actual heavy crude oil: Theoretical optimization and experimental
19
20 evaluation, *Process Safety and Environmental Protection*, 136, 334–342.
21
22

23
24
25
26 [2] Banković-Ilić, I.B., Stamenković, O.S., Veljković, V.B., 2012. Biodiesel
27
28 production from non-edible plant oils. *Renewable and Sustainable Energy Reviews*
29
30 16, 3621– 3647.
31
32

33
34
35
36 [3] Takase, M., Zhang, M., Feng, W., Chen, Y., Zhao, T., Cobbina, S.J., Yang, L.,
37
38 Wu, X., 2014. Application of zirconia modified with KOH as a heterogeneous solid
39
40 base catalyst to new non-edible oil for biodiesel. *Energy Conversion and Management*
41
42 80, 117–25.
43
44

45
46 [4] Sharma, Y.C.; Singh, B.; Upadhyay, S.N. Advancements in development and
47
48 characterization of biodiesel: A review. *Fuel* 2008, 87, 2355–2373.
49

50
51 [5] Lee, J.S.; Saka, S. Biodiesel production by heterogeneous catalysts and
52
53 supercritical technologies. *Bioresour. Technol.* 2010, 101, 7191–7200.
54
55
56
57
58
59
60
61
62
63
64
65

- 1
2
3
4 [6] Arzamendi, G., Campo, I., Arguiñarena, E., Sánchez, M., Montes, M., Gandía,
5 L.M., 2007. Synthesis of biodiesel with heterogeneous NaOH/alumina catalysts:
6 Comparison with homogeneous NaOH. Chemical Engineering Journal 134, 123–30.
7
8
9
10
11 [7] Aidan M. Doyle, Talib M. Albayati, Ammar S. Abbas, Ziad T. Alismaeel, 2016.
12 Biodiesel production by esterification of oleic acid over zeolite Y prepared from
13 kaolin. Renewable Energy; 97:19-23.
14
15
16
17 [8] Marciniuk, L.L., Hammerb, P., Pastore, H.O., Schuchardt, U., Cardoso, D., 2014.
18 Sodium titanate as a basic catalyst in transesterification reactions. Fuel 118, 48–54.
19
20
21 [9] Salinas, D., Guerrero, S., Cross, A., Araya, P., Wolf, E.E., 2016. Potassium
22 titanate for the production of biodiesel. Fuel 166, 237–244.
23
24
25
26 [10] Talib M. Albayati, Sophie E. Wilkinson, Arthur A. Garforth & Aidan M. Doyle.
27 Heterogeneous Alkane Reactions over Nanoporous Catalysts. Transport in Porous Media, Volume
28 104, No. 2 (2014); Pages; 315-333. DOI 10.1007/s11242-014-0336-1.
29
30
31 [11] Talib M. Albayati and Aidan M. Doyle. "SBA-15 Supported Bimetallic Catalysts for
32 Enhancement Isomers Production During n-Heptane Decomposition" International Journal of
33 Chemical Reactor Engineering, 12(1) (2014)345–354. DOI: 10.1515/ijcre-2013-0120.
34
35
36 [12] Feyzi, M., Shahbazi, Z., 2017. Preparation, kinetic and thermodynamic studies
37 of Al–Sr nanocatalysts for biodiesel production. Journal of the Taiwan Institute of
38 Chemical Engineers 71, 145-155.
39
40
41 [13] Han, H., Guan, Y., 2009. Synthesis of biodiesel from rapeseed oil using K₂O/γ-
42 Al₂O₃ as nano–solid–base catalyst. Wuhan University Journal of Natural Science 14,
43 75–9.
44
45
46
47
48
49
50
51
52
53
54
55
56
57
58
59
60
61
62
63
64
65

- 1
2
3
4 [14] Feyzi, M., Norouzi, L., 2016. Preparation and kinetic study of magnetic
5 Ca/Fe₃O₄@SiO₂ nanocatalysts for biodiesel production. *Renewable Energy* 94, 579-
6
7 586.
8
9
10
11 [15] Faria, E.A., Marques, J.S., Dias, I.M., Andrade, R.D.A., Suarez, P.A.Z., Prado,
12 A.G.S., 2009. Nanosized and reusable SiO₂/ZrO₂ catalyst for highly efficient
13 biodiesel production by soybean transesterification. *Journal of Brazilian Chemical*
14 *Society* 20, 1732–7.
15
16
17
18
19 [16] Zhou, Q., Zhang, H., Chang, F., Li, H., Pan, H., Xue, W., De-Yu, H., Yang, S.,
20 2015. Nano La₂O₃ as a heterogeneous catalyst for biodiesel synthesis by
21 transesterification of *Jatropha curcas* L. *Oil. J Indus Eng Chem* 31, 385-392.
22
23
24 [17] Abbas, A. S., & Abbas, R. N. (2013). Kinetic study and simulation of oleic acid
25 esterification over prepared NaY zeolite catalyst. *Iraqi Journal of Chemical and*
26 *Petroleum Engineering*, 14(4), 35-43.
27
28
29 [18] Abbas, A. S., & Abbas, R. N. (2015). Preparation and Characterization of NaY
30 Zeolite for Biodiesel Production. *Iraqi Journal of Chemical and Petroleum*
31 *Engineering*, 16(2), 19-29.
32
33
34 [19] Abbas, A.S.; Albayati, T.M.; Alismael, Z.T.; Doyle, A.M.: Kinetics and mass
35 transfer study of oleic acid esterification over prepared nanoporous HY zeolite. *IJCPE*
36 17(1), 47–60 (2016)
37
38
39 [20] Alfattal, A. H., & Abbas, A. S. (2019). Synthesized 2nd Generation Zeolite as an
40 Acid- Catalyst for Esterification Reaction. *Iraqi Journal of Chemical and Petroleum*
41 *Engineering*, 20(3), 67-73. <https://doi.org/10.31699/IJCPE.2019.3.9>.
42
43
44
45
46
47
48
49
50
51
52
53
54
55
56
57
58
59
60
61
62
63
64
65

- 1
2
3
4 [21] Alshahidy, B. A., Abbas, A. S. (2020). Preparation and modification of 13X
5 zeolite as a heterogeneous catalyst for esterification of oleic acid. AIP Conference
6 Proceedings 2213, 020167 (2020); <https://doi.org/10.1063/5.0000171>.
7
8
9
10
11 [22] Alshahidy, B. A., Abbas, A. S. (2021). Comparative Study on the Catalytic
12 Performance of a 13X Zeolite and its Dealuminated Derivative for Biodiesel
13 Production. Bulletin of Chemical Reaction Engineering & Catalysis, 16 (4), 763-772
14 (doi:10.9767/bcrec.16.4.11436.763-772).
15
16
17
18
19
20
21 [23] Qasim, D., Abdul-Aziz, Y. I., & Alismaeel, Z. T. (2019). Biodiesel from fresh
22 and waste sunflower oil using calcium oxide catalyst synthesized from local
23 limestone. Res. J. Chem. Environ, 23, 111-119.
24
25
26
27
28 [24] Baskar, G., Gurugulladevi, A., Nishanthini, T., Aiswarya, R., Tamilarasan, K.,
29 2017. Optimization and kinetics of biodiesel production from Mahua oil using
30 manganese doped zinc oxide nanocatalyst. Renewable energy, 103, 641-646.
31
32
33
34
35 [25]. K. Ankur, W. Karen, F.L. Adam, S. Jhuma, Kinetic modelling studies of
36 heterogeneously catalyzed biodiesel synthesis reactions, Ind. Eng. Chem. Res.50
37 (2011) 4818–4830.
38
39
40
41
42 [26]. E.G. Al-Sakkari, S.T. El-Sheltawy, N.K. Attiab, S.R. Mostafa, Kinetic study of
43 soybean oil methanolysis using cement kiln dust as a heterogeneous catalyst for
44 biodiesel production. Applied Catalysis B: Environmental 206 (2017) 146–157.
45
46
47
48
49 [27]. L. Hsieh, U. Kumar, J.C.S. Wu, Continuous production of biodiesel in a packed-
50 bed reactor using shell–core structural $\text{Ca}(\text{C}_3\text{H}_7\text{O}_3)_2/\text{CaCO}_3$ catalyst. Chem. Eng. J.
51 158 (2010) 250–256.
52
53
54
55
56
57
58
59
60
61
62
63
64
65

- 1
2
3
4 [28]. Dossin, T. F., Reyniers, M. F. and Marin, G. B., “Kinetics of heterogeneously
5
6 MgO-catalyzed transesterification”, Applied Catalysis B: Environmental, Vol. 62, pp.
7
8 35-45, 2006.
9
- 10
11 [29]. A. Chantrasa, N. Phlernjai, J.G. Goodwin, Kinetics of hydrotalcite catalyzed
12
13 transesterification of tricaprylin and methanol for biodiesel synthesis. Chem. Eng. J.
14
15 168 (2011) 333–340.
16
17
- 18
19 [30] Nouredini and Zhu D., “Kinetics of transesterification of soybean oil”, Journal
20
21 of American oil chemical society, vol. 74, no. 11, pp.1457–1463, 1997.
22
23
- 24 [31] Vicente, G., Martínez, M., Aracil, J. and Esteban, A., “Kinetics of sunflower oil
25
26 methanolysis”, Industrial and Engineering Chemistry Research, vol. 44, no.15 pp.
27
28 5447-5454, 2005.
29
- 30
31 [32] Klofutar, B. and Golob, J., “The transesterification of rapeseed and waste
32
33 sunflower oils: Mass-transfer and kinetics in a laboratory batch reactor and in an
34
35 industrial scale reactor/separator setup”, Bioresource Technology, vol. 101, No. 10,
36
37 pp. 3333-3344, 2010.
38
39
- 40
41 [33] Zanjani, N., Pirzaman A. and Yazdanian E., “Biodiesel production in the
42
43 presence of heterogeneous catalyst of alumina: Study of kinetics and
44
45 thermodynamics”, International Journal of Chemical Kinetics, vol. 52, No. 7, pp. 472-
46
47 484, 2020.
48
49
- 50
51 [34] Dhawane S., E.G.Al-Sakkari, Kumar T. and Halder G., “Comprehensive
52
53 elucidation of the apparent kinetics and mass transfer resistances for biodiesel
54
55 production via in-house developed carbonaceous catalyst”, Chemical Engineering
56
57 Research and Design, 2020.
58
59
60
61
62
63
64
65

- 1
2
3
4 [35] Doyle AM, Alismaeel, ZT, Albayati TM, Abbas AS, “High purity FAU-type
5 zeolite catalysts from shale rock for biodiesel production” Fuel vol. 199 pp. 394–402,
6
7
8
9 2017.
- 10
11 [36] Z.T. Alismaeel, A.S. Abbas, T.M. Albayati, A.M. Doyle, “Biodiesel from batch
12 and continuous oleic acid esterification using zeolite catalysts” Fuel vol. 234 pp.170–
13
14
15
16
17 176, 2018.
- 18
19 [37] Albayati, T.M., Doyle, A.M., “Encapsulated heterogeneous base catalysts onto
20
21
22
23
24
25
26
27
28
29
30
31
32
33
34
35
36
37
38
39
40
41
42
43
44
45
46
47
48
49
50
51
52
53
54
55
56
57
58
59
60
61
62
63
64
65
- [38] Encinar J. M., González J. F., Martínez G. and Sánchez N., “Synthesis and
characterization of biodiesel obtained from castor oil transesterification”,
International Conference on Renewable Energies and Power Quality, Spain, 2010.
- [39] Viele, E. L, Chukwuma, F. O. and Uyigue, L. “Production and Characterization
of Biodiesel from crude Palm Kernel Oil and Bio-ethanol using Potash from Ash of
Empty Oil Palm Bunch Residue as Catalyst”, IJAIEM, Volume 3, Issue 1, pp. 355-
363, 2014.
- [40] Satterfield C.N., “Heterogeneous catalysis in industrial practice”, 2nd Edition,
McGraw-Hill, New York, pp. 53-68, 1991.
- [41] Lina Zhao, “Novel Solid Base Catalysts for the Production of Biodiesel from
Lipids”, thesis, University of Kansas School of Engineering, 2010.
- [42] Xiao, Y., Gao, L., Xiao, G. and Lv, J., “Kinetics of the transesterification reaction
catalyzed by solid base in a fixed-bed reactor”, Energy & Fuels, vol. 24, no. 11, pp.
5829-5833, 2010.

- 1
2
3
4 [43]. H. Hattori, M. Shima, H. Kabashima, Alcoholysis of ester and epoxide catalyzed
5
6 by solid bases, *Stud. Surf. Sci. Catal.* 130 (2000) 3507–3512.
7
8
9 [44] M. Di Serio, M. Ledda, M. Cozzolino, G. Minutillo, R. Tesser, and E.
10 Santacesaria, “Transesterification of soybean oil to biodiesel by using heterogeneous
11 basic catalysts,” *Industrial and Engineering Chemistry Research*, vol. 45, no. 9, pp.
12 3009–3014, 2006.
13
14 [45]. Khairi R. Kalash, Talib M. Albayati, Remediation of oil refinery wastewater implementing
15 functionalized mesoporous materials MCM-41 in batch and continuous adsorption process,
16 *Desalination and Water Treatment* 220 (2021) 130-141. [https:// doi: 10.5004/dwt.2021.27004](https://doi.org/10.5004/dwt.2021.27004).
17
18 [46] Haneen F. Alazzawi, Issam K. Salih, Talib M. Albayati, Drug delivery of amoxicillin
19 molecule as a suggested treatment for covid-19 implementing functionalized mesoporous SBA-15
20 with aminopropyl groups. *Drug Delivery*, 28 (1) (2021) 856–864.
21 <https://doi.org/10.1080/10717544.2021.1914778>.
22
23 [47] Endalew AK, Kiros Y and Zanzi R, “Inorganic heterogeneous catalysts for
24 biodiesel production from vegetable oils”, *Biomass Bioenergy*, Vol. 35, pp. 3787-
25 3809, 2011.
26
27 [48] Najafpour G. D., Hassani M., Mohammadi M. and Rabiee M., “Preparation,
28 Characterization of Biodiesel from Waste Cooking Oil”, *Journal of Scientific &*
29 *Industrial Research*, vol. 73, pp. 129-133, 2014.
30
31 [49] Noiroj .K., Intarapong P., Luengnaruemitchai A. and Jai-In S., “A comparative
32 study of KOH/Al₂O₃ and KOH/NaY catalysts for biodiesel production via
33 transesterification from palm oil”, *Renewable Energy* 34, pp. 1145–1150, 2009.
34
35
36
37
38
39
40
41
42
43
44
45
46
47
48
49
50
51
52
53
54
55
56
57
58
59
60
61
62
63
64
65

- 1
2
3
4 [50] Hill, C. G. Jr., "An Introduction to chemical engineering kinetics and reactor
5 design", John Willy and Sons, 1977.
6
7
8
9 [51] Tiwari AK, Kumar A. and Raheman H., "Biodiesel production from jatropha oil
10 (Jatropha curcas) with high free fatty acids: an optimized process". Biomass
11 Bioenergy, vol.31, pp.569–75, 2007.
12
13
14 [52] J. M. Encinar, J. F. González and A. Rodríguez-Reinares, "Biodiesel from Used
15 Frying Oil. Variables Affecting the Yields and Characteristics of the Biodiesel", in
16 Industrial & Engineering Chemistry Research, (2005), Vol. 44, pp. 5491-5499.
17
18
19 [53] Titipong I., "Development of Biodiesel Production Processes from Various
20 Vegetable Oils", thesis, University of Saskatchewan, 2011.
21
22
23 [54] Arjun B. C., K. C. W. and Rafiqul M. I., "Waste Cooking Oil as an Alternate
24 Feedstock for Biodiesel Production", Energies, 1, pp. 3-18, 2008.
25
26
27 [55] Vicente G.; Martinez, M.; Aracil J., "Optimization of integrated biodiesel
28 production", Bioresour Technol., vol.98, pp.1724-1733, 2007.
29
30
31 [56] Lang, X.; Dalai, A.K.; Bakhsi, N.N.; Reaney, M.J.; Hertz, P.B. "Preparation and
32 characterization of bio-diesels from various bio-oils". Bioresource Technology, vol.
33 80, pp. 53-62, 2001.
34
35
36 [57] Beatrice O. O., Onyia1 O. C. and Abdulraman F.W., "Production of biodiesel
37 from used vegetable oil", G.J.B.A.H.S., Vol.3, No.1, pp. 274-277, 2014.
38
39
40
41
42
43
44
45
46
47
48
49
50
51
52
53
54
55
56
57
58
59
60
61
62
63
64
65

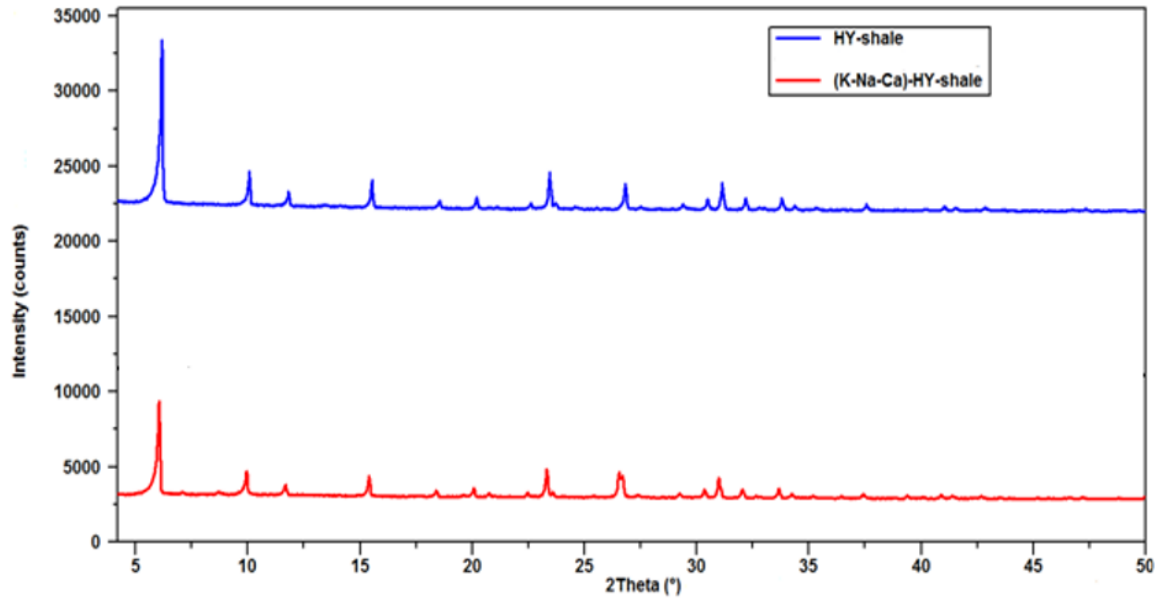


Figure 1: XRD Patterns of two Configurations of HY-shale Zeolite

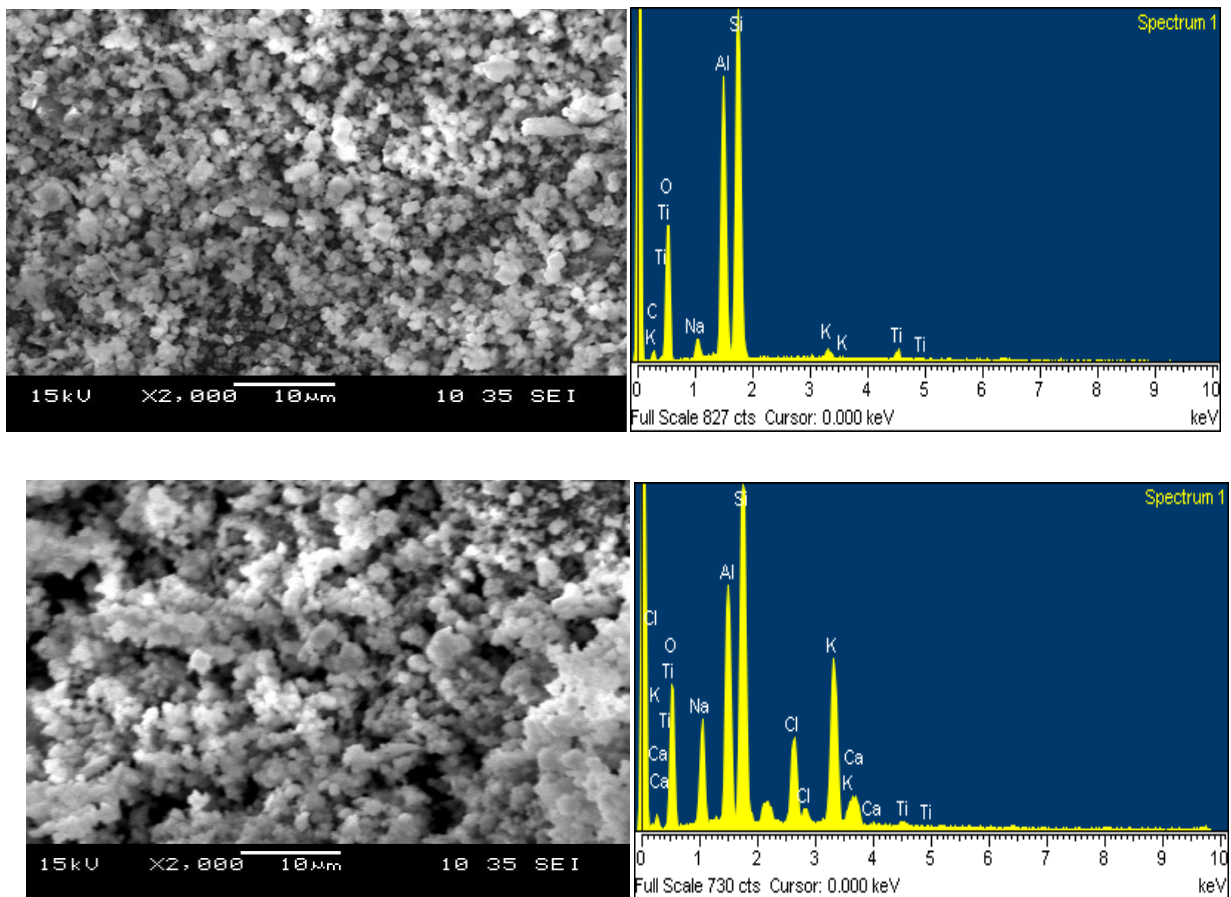


Figure 2: SEM and EDAX images for H-FAU (top) and Ca-Na-K-FAU (bottom).

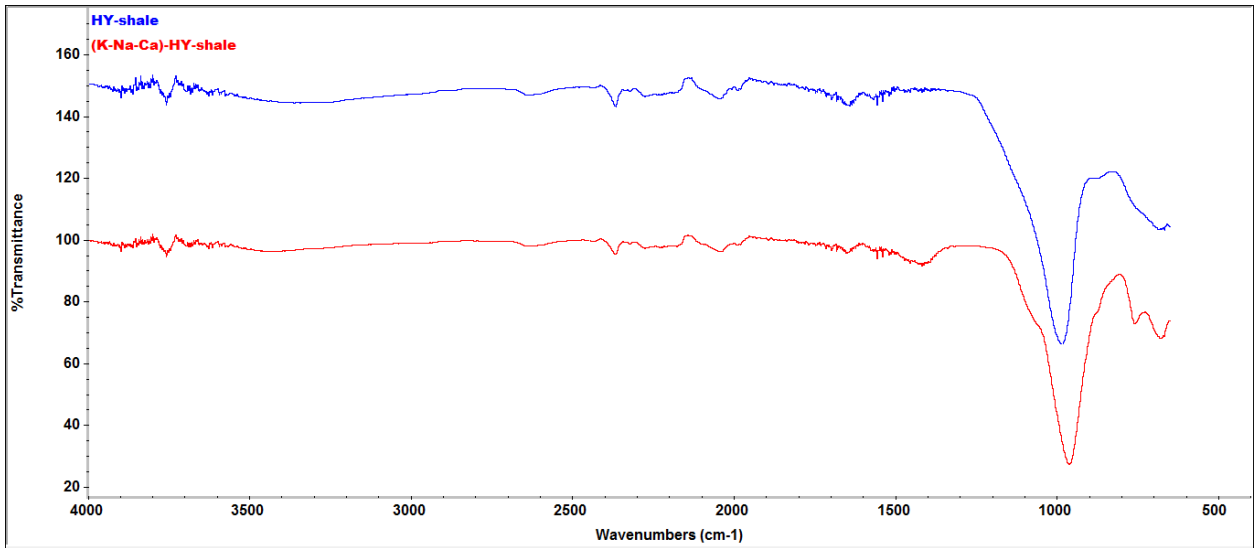


Figure 3: FTIR test for HY-shale (top) and (K-Na-Ca)-HY shale (bottom).

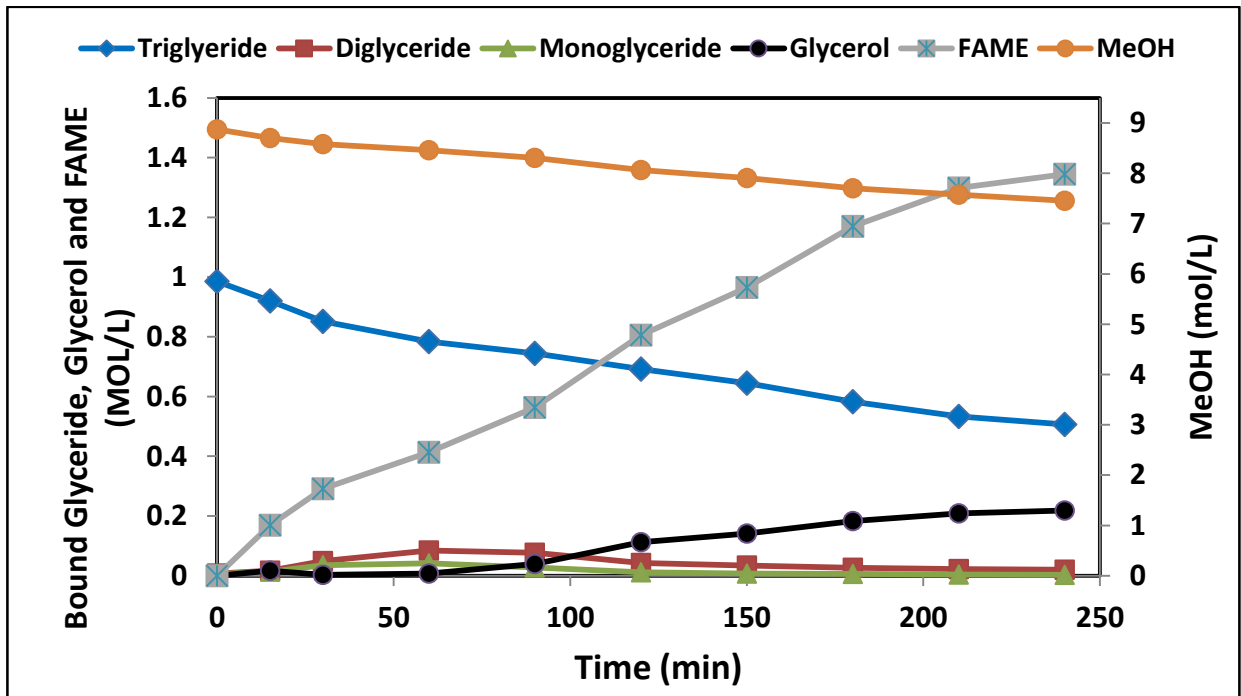


Figure 4: Concentration-Time Plot for Transesterification Using H-FAU Zeolite

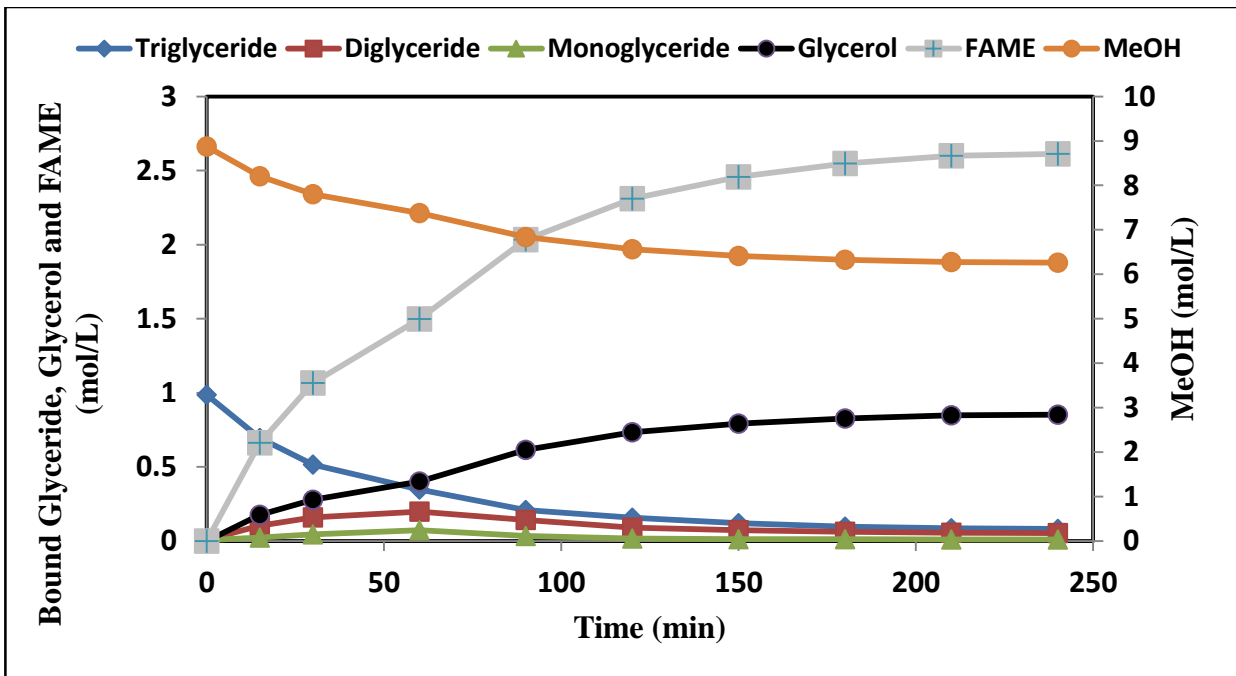


Figure 5: Concentration-Time Plot for Transesterification using Na-K-Ca-FAU Zeolite

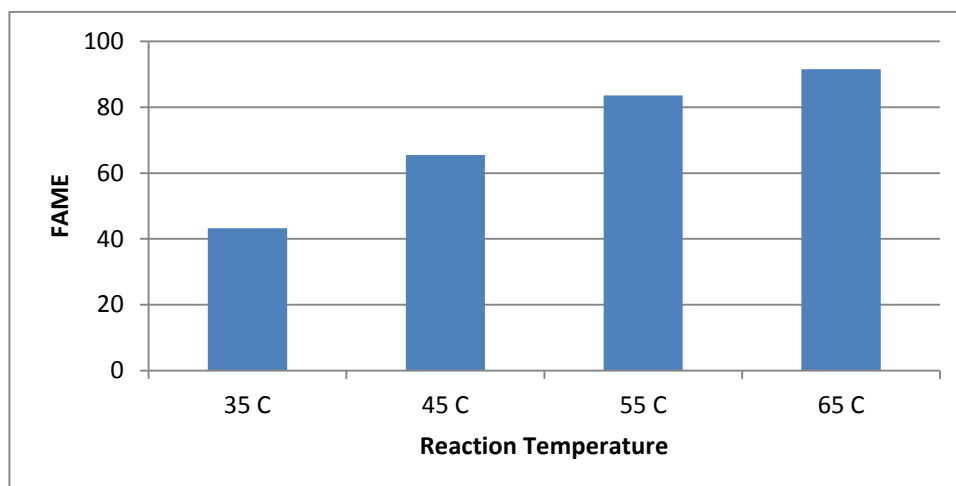


Figure 6: Effect of Temperature on FAME Content using Catalyst Concentration 5% and meth/oil 9:1

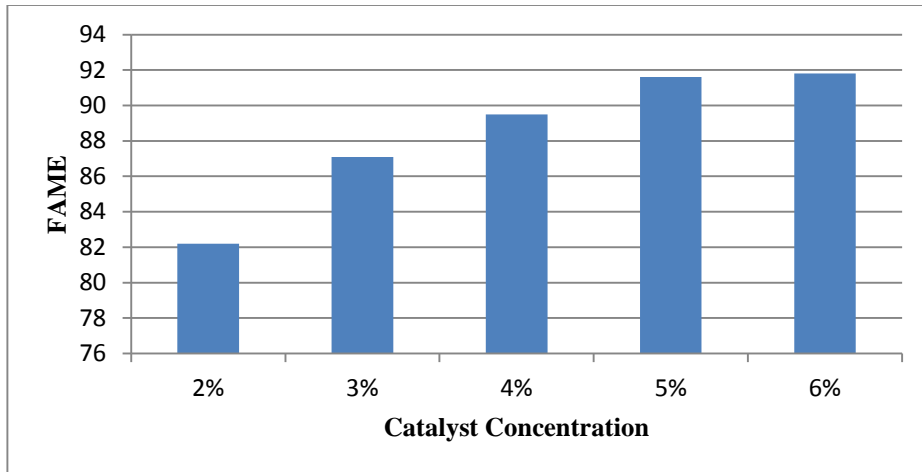


Figure 7: Effect of catalyst Concentration on FAME Content using meth/oil =9:1 and Temperature 65C°

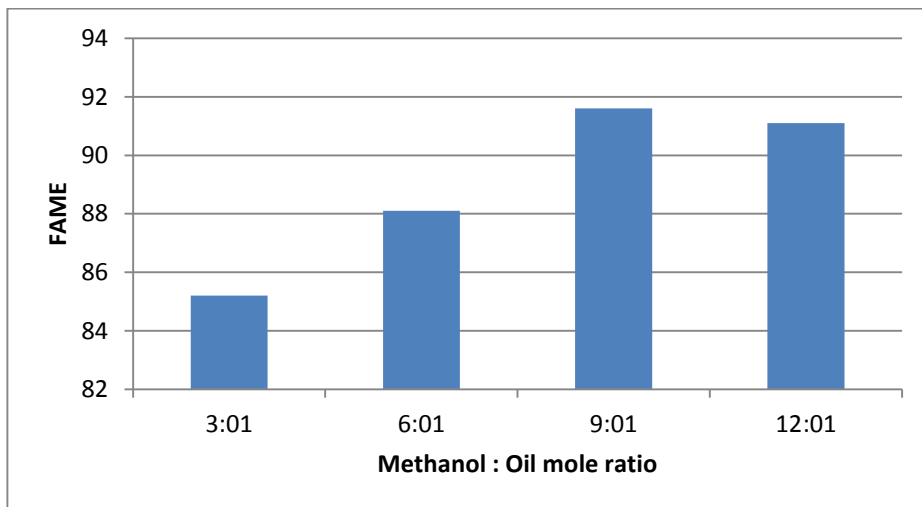
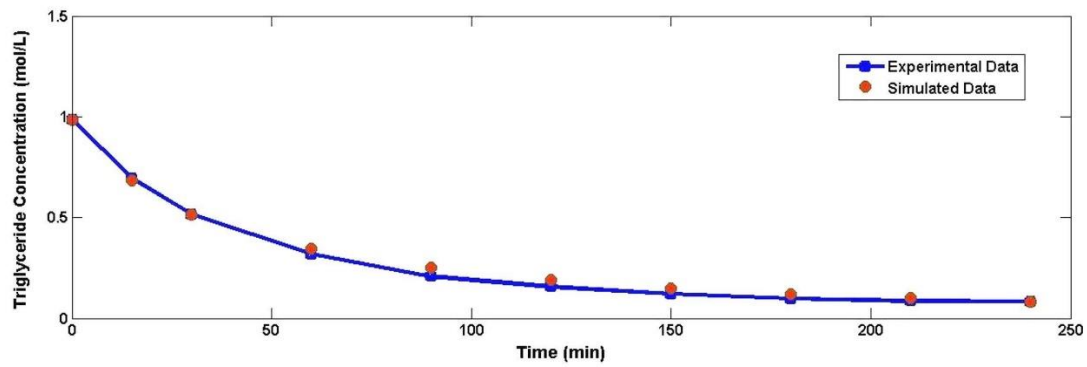
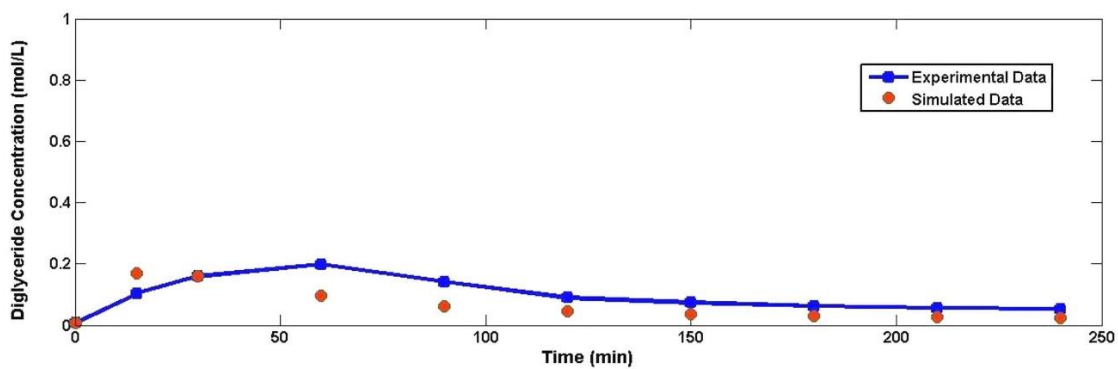


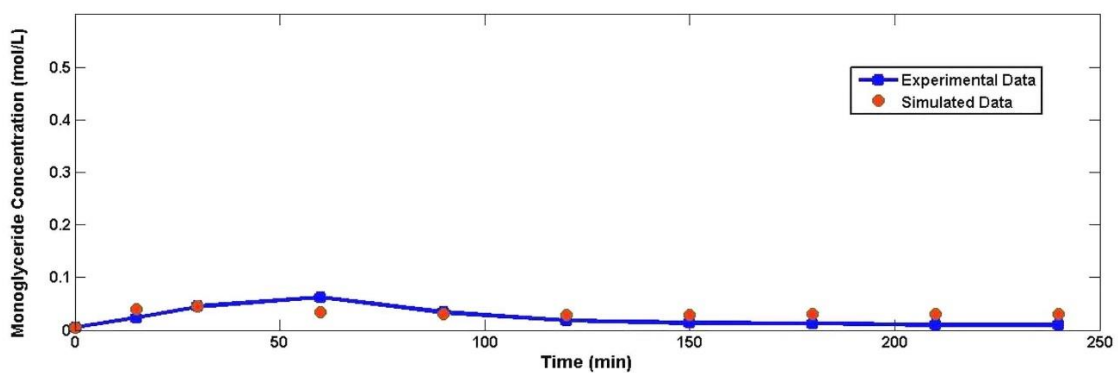
Figure 8: Effect of meth/oil on FAME Content using Catalyst Concentration 5% and Temperature 65C°



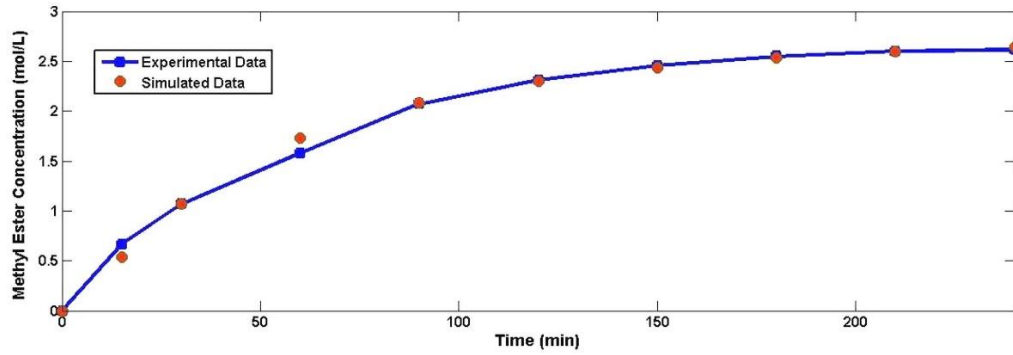
(a)



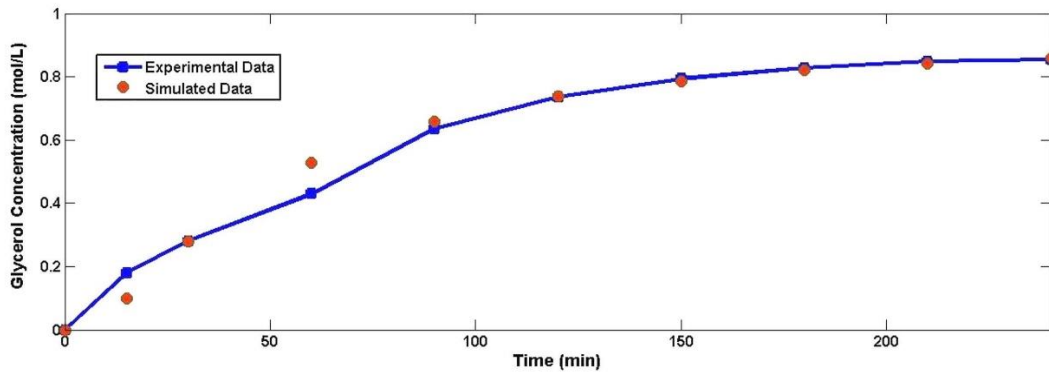
(b)



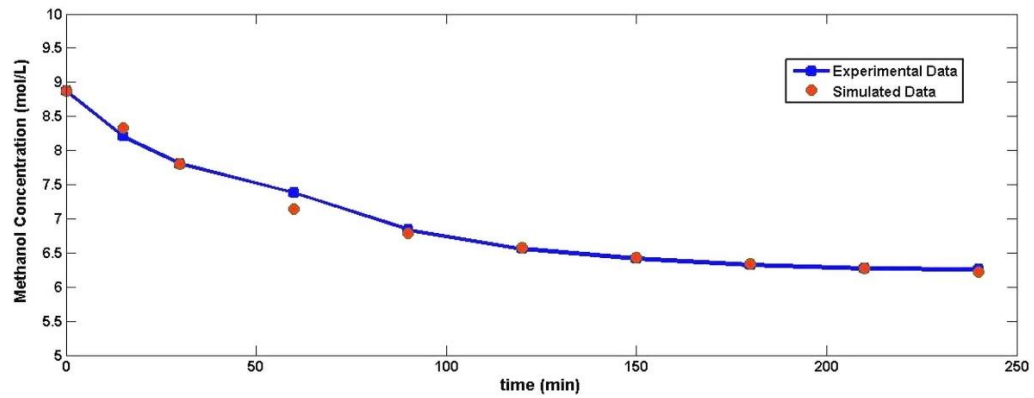
(c)



(d)



(e)



(f)

Figure 9: Dynamic Behavior Comparison between Experimental Work and Simulated Data for Different Product Concentrations

- (A) For Triglyceride Concentration
- (B) For Diglyceride Concentration
- (C) For Monoglyceride Concentration
- (D) For Methyl ester Concentration
- (E) For Glycerol Concentration
- (F) For Methanol Concentration

Table (1): Physicochemical Properties of two HY-shale Zeolite Configurations

Catalyst	Surface Area (A_{BET}) (m^2/g)	Pore Volume (V_p) (cm^3/g)	Pore Size (D_p) (nm)
H-FAU	571.3	0.73	13.6
Na-K-Ca-FAU	325.5	0.54	9.7

Table (2): The Constant Values of all Types of Oils

Type of oil	Constant	
	(a)	(b)
glycerol	0.909	-0.01
Monoglyceride	0.723	0.281
diglyceride	0.956	0.013
triglyceride	2.667	0.038

Table (3): Optimal Value of the Constants for Transesterification Rate Reaction

Reaction Rate Constant	Present work ($L.mol^{-1}min^{-1}$)	Work was done by Nouredini and Zhu (1997) [30]	Work was done by Vicente <i>et al.</i> 2005 [31]	Work was done by Klofutar and Golob (2010) [32]
k_1	0.0029	0.050	0.00510	0.09
k_2	0.0183	0.110	0.398	0.5
k_3	0.0092	0.215	0.542	0.156
k_4	0.0108	1.228	0.958	0.1
k_5	0.0344	0.242	0.009	0.7
k_6	0.0027	0.007	0.000015	0.0061

Table (4): Specification of the Biodiesel Production

Specification	Biodiesel from Present work.	Biodiesel by Arjun, <i>et al.</i> , (2008) [49]	ASTM (D6751)	
			Method	Limit
Specific gravity (15.6° C), g/cm ³	0.91	0.87	D-941	0.86 to 0.9
°A.P.I Gravity *	23.99	31.14	D-941	0 to 100
Kinematic Viscosity 40° C (mm ² /s)	4.286	5.03	D-445	1.9 to 6.0
Rams bottom Carbon Residue (RCR),wt. %	0.0832	-----	D-524	0.05 max
Aniline Point (°C)	86.257 187.26 F	-----	D-611	25 to 130
Diesel Index (DI)**	44.92	-----	-----	45 to 55
Cetane No. (min)	57.6	61	D-613	48 to 60
Cloud Point (°C)	2	-1	D-2500	-3 to 12
Pour Point (°C)	-3	-16	D-97	-15 to 16
Flash Point (°C)	151	164	D-93	100 to 170

* A.P.I = (141.5/Specific gravity. at 15.6° C) – 131.5

** DI. = (A.P.I * Aniline point/100), [52].